

# ASSESSMENT OF REDUCED ORDER FUSELAGE AND BLADE MODELS FOR ROTORCRAFT INTERACTIONAL AERODYNAMICS

Stéphanie Péron<sup>1</sup>, Dylan Jude<sup>2</sup>, Andrew Wissink<sup>2</sup>, and Ronan Boisard<sup>1</sup>

<sup>1</sup>*DAAA, ONERA, Université Paris Saclay, F-92322 Châtillon, France*

<sup>2</sup>*U.S. Army Combat Capabilities Development Command, Aviation & Missile Center, Moffett Field, CA 94035, USA*

\* *Corresponding author: stephanie.peron@onera.fr*

## Abstract

This paper investigates mid-fidelity Cartesian-based CFD tools developed either by the U.S. Army and ONERA for rotorcraft aerodynamics in the framework of the US-France Project Agreement on Rotary Wing Aeromechanics and Human Factors Integration Research. The common test-case is the simulation of the interaction between the rotor and the fuselage of the D365N configuration in forward flight, for which high-fidelity CFD simulations have been conducted in 2009. US Army's code Helios/ROAM models the fuselage with an immersed boundary method (IBM) and the rotor blades as an actuator line. ONERA's code FAST also models the fuselage with an IBM representation and the blades using body-fitted overset grids. This work presents a comparison of fuselage loads, rotor loads, and wake between simulations and experiments.

## 1. INTRODUCTION

Prediction of aircraft aerodynamics is a key component in the rotorcraft design process. Rotorcraft comprehensive analysis tools, such as RCAS<sup>1</sup> and HOST,<sup>2</sup> are tightly integrated into the design process of a new rotorcraft. However their aerodynamic models for the rotor and fuselage are often low-fidelity. For traditional, single-main-rotor helicopters, a low-fidelity model tuned for certain flight conditions may produce adequate results for the purposes of design. Modern rotorcraft configurations, however, often include multiple rotors and lifting surfaces with non-trivial interactional aerodynamics and low-fidelity models often cannot account for these factors. For the design process to include effects of complex interactional aero-

dynamics, higher-fidelity aerodynamic models need to be introduced into the design loop.

At the opposite end of the spectrum from low-fidelity aerodynamic lies high-fidelity, computationally expensive tools using overset Computational Fluid Dynamics (CFD). Codes such as *e/sA*<sup>3</sup> (ONERA) and Helios<sup>4,5</sup> (CREATE<sup>TM</sup>-AV) are established, accurate CFD frameworks for simulating complex aerodynamics. Both frameworks use a "Chimera" approach by which unstructured, structured curvilinear, or strand near-body meshes are overset within a Cartesian background mesh. The near-body meshes resolve the near-wall viscous boundary-layer flow and the off-body Cartesian region prescribes Adaptive Mesh Refinement (AMR) to resolve aircraft or rotor wakes and inter-

actional aerodynamics. A Helios or *e/sA* simulation of an aircraft will commonly have tens or hundreds-of-millions of degrees of freedom, requiring parallel execution on a large scale high performance computing (HPC) supercomputer. Even with thousands of CPU cores on modern supercomputers, complex simulations can still take days or weeks to complete.

Research groups at ONERA and the US Army have recently developed mid-fidelity tools intended to fill the gap between the traditional low and high-fidelity tools available today. Specifically, these tools are designed to give reasonably accurate aerodynamic loads analysis of the interactional aerodynamics experienced by modern rotorcraft vehicles but at a much faster turnaround rate than high-fidelity overset body-fitted CFD methods. In both models, complex geometries that would normally require large near-body grids are replaced with an immersed boundary representation. The Immersed Boundary Method (IBM) interacts directly with the background Cartesian mesh to inject influence from body so that interactional effects are captured. Since viscous body-fitted meshes are not required, solutions are performed only on computationally-efficient Cartesian grids. Further, larger timesteps are allowed through elimination of cell size limitations of viscous boundary layer meshes. The combination of these two features enable accelerations of up to 40X-50X faster over traditional high-fidelity overset CFD methods.

The IBM approach does not work well for modeling rotor blades or other lifting surfaces without very fine Cartesian refinement. Helios solves this problem by representing each blade as an actuator line. Sectional loads based on 2D aerodynamics are integrated along the blade span and injected into the background Cartesian mesh as source terms in the governing Navier–Stokes equations.

The IBM and actuator line methods in

Helios are implemented in a module called the Reduced Order Aerodynamic Model (ROAM). ROAM is used in Helios alongside a Cartesian solver, either SAMCart or Orchard. For this work, only the octree-based AMR solver Orchard<sup>5</sup> is used as the background Cartesian solver.

ONERA considers a different approach within FAST/Cassiopee framework: URANS solution is computed on wall-resolved curvilinear grids describing the blades, in relative motion with respect to the off-body Cartesian mesh, in which the fuselage is modeled by IBM. A wall function is applied to recover the skin friction onto the fuselage, as detailed in Péron *et al.*<sup>6</sup> and Constant *et al.*<sup>7</sup>. The present study investigates the usage of Helios/ROAM and FAST/IBM to assess interactional aerodynamics of the 7A four-bladed rotor on the Dauphin fuselage (D365N test case) for which existing body-fitted CFD results are available<sup>8</sup>.

## 2. DESCRIPTION OF THE TEST-CASE

A scaled model of the Dauphin helicopter equipped with a powered main rotor was designed and tested in the late 1980s in the ONERA S2Ch wind tunnel and in ONERA F1 subsonic wind tunnel. The test provided experimental data, including steady and unsteady fuselage surface pressures, balance measurements, 2D and 3D PIV wake measurements. The tested helicopter model is a 1/7.7 Dauphin model with a 1.5 meter fuselage. The powered main rotor is a 0.75 meter radius 4-bladed rotor articulated in pitch, flap and lead-lag motions. The 0.05 m constant chord blade uses OA209 airfoils and has -12 deg/R of linear twist. The blade root cutout is at 0.275R. The clockwise rotor rotation is ensured by an electric engine which allows a blade tip speed of  $100 \text{ m}\cdot\text{s}^{-1}$  (1272 RPM). The F1 experimental fuselage model varies from the theoretical Dauphin 365N model definition, especially in the area of the engine inlet and exhaust fairings. Neither the

tail rotor nor the rotor hub are included in the present simulations; the strut and wind tunnel walls have also been excluded.

In the F1 experiments, the D365N configuration is trimmed to a specific thrust ( $Z_b=14.5$ ), axial force ( $X_b=0$ ) and rotor lateral flapping  $\beta_{1s}=0$ . The baseline flow conditions are  $V_\infty=15 \text{ m}\cdot\text{s}^{-1}$ , corresponding to a Mach number  $Ma_\infty=0.044$  and a moderate advance ratio  $\mu = 0.15$ ,  $-3^\circ$  fuselage angle of attack and zero sideslip, well suited for the study of the rotor-fuselage interaction, as the rotor wake impinges the fuselage and the empennage. The Reynolds number is 1.07 million per meter. The rotor control angles (collective, flap, lag and harmonics) are obtained from the rotorcraft comprehensive code HOST<sup>2</sup>. Rigid blade deflections are applied about lag and flap hinges using three harmonics.

### 3. COMPUTATIONAL FRAMEWORK

#### 3.1. Helios ROAM

Helios<sup>4</sup> is a high-fidelity coupled CFD/CSD infrastructure dedicated to aeromechanics predictions of rotorcraft. It relies traditionally on body conforming unstructured or structured-curvilinear meshes in the near-body region and Cartesian meshes in the off-body region. The near-body grids rotate, move, and deform with the rotor blades and resolve the unsteady turbulent viscous scales in the boundary layer. The stationary off-body Cartesian solver resolves the wake through a combination of AMR and high-order accurate discretizations. Data transfer between the two mesh systems are performed through the use of overset domain connectivity transfer technology that dynamically cuts holes and fringes in the meshes to accommodate the relative motion between the mesh systems. Typical simulations may require several days on HPC systems while larger simulations requiring many rotor revolutions may take over a week to complete.

A medium-fidelity option has recently been implemented in Helios, named ROAM (Reduced-Order Aerodynamics Model), relying on Cartesian grids<sup>4</sup>. It applies an actuator line model for the rotor and an immersed boundary representation of the fuselage. The Cartesian solver used by ROAM is the same off-body solver used to resolve the wake in near-body/off-body overset calculations in Helios. Calculations with ROAM are significantly faster than the traditional body-fitted calculations for two reasons; 1) it avoids the cost of near-body viscous boundary layer solution and domain connectivity because it does not explicitly resolve this region; and 2) it allows for much larger timesteps in the unsteady simulation.

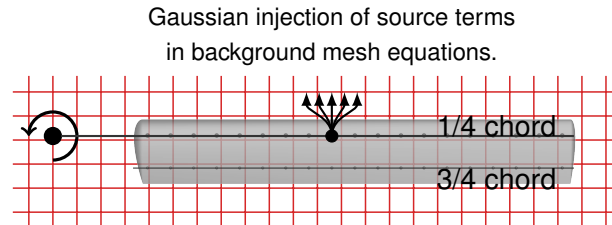


Figure 1: Illustration of actuator line implementation to simulate a rotor blade using the injections of source terms from sectional loads.

The methodology for using actuator lines in ROAM is based on lifting-line theory and similar to the approaches from by Mittal *et al.*<sup>9</sup> and Churchfield *et al.*<sup>10</sup>. A lifting line along the blade is discretized into a set of control points and the flow induced velocities at these control points are interpolated from the Cartesian mesh system modeling the flow field. To exclude the effects of bound circulation, a circle of sensors is created around each control point and the velocity at the control point is found as an average of all sensors. Once the velocities at control points are obtained, linear aerodynamic theory augmented with airfoil tables are used to determine the force coefficients and compute the force distribution. The force distribution is then embedded into the flow field

equations as source terms for the momentum and energy equations. An illustration of the lifting line in a background mesh is shown in Fig. 1. The normal component of the resultant force is injected back into the domain at both the 1/4 and 3/4 chord locations in proportions to match the aerodynamic pitching moment at that span-wise section.

Helios has two background Cartesian AMR solvers available for use. SAMCart uses patch-based refinement and Orchard uses an octree-based data structure for refinement. The underlying numerics for the Cartesian Navier–Stokes equation are the same between both approaches, however the octree-based approach in Orchard results in performance and scalability improvements over SAMCart. For all Helios cases in this work Orchard is used as the background Cartesian solver. The inviscid terms of the Navier–Stokes equations use a 5<sup>th</sup>-order central stencil with scalar dissipation and the viscous terms use 4<sup>th</sup>-order stencils. The temporal order of accuracy is second order using an implicit backwards differencing algorithm with dual-timestepping. Some high-fidelity results in this work are obtained for reference from Helios using body-fitted and the mStrand<sup>11</sup> solver overset in a similar background domain.

### 3.2.FAST/IBM

FAST solver<sup>12</sup> is a structured multi-block Finite-Volume solver devoted to high-fidelity simulations (including DNS, LES and RANS-LES simulations), developed by ONERA. Current FAST architecture relies on an hybrid MPI/OpenMP parallelism on CPUs and is integrated within a CGNS/Python framework in combination with Cassiopee set of modules for pre, co- and post-processing<sup>13</sup>, providing a versatile simulation tool to perform either high-fidelity unsteady simulations on structured multi-block meshes, Cartesian IBM meshes, and more recently hybrid IBM and body-fitted meshes together. FAST Cartesian solver is applied on Carte-

sian grids, dividing by two the memory and CPU time compared to the curvilinear solver.

An overset grid capability for rotorcraft applications has been recently developed within Cassiopee and applied with FAST solver. For that range of applications, curvilinear grids are defined around rotor blades whereas the off-body region is meshed by an octree-like Cartesian mesh, as described in Péron *et al.*<sup>14</sup>. For that purpose, Chimera transfers are performed at each sub-time step between curvilinear grids and Cartesian grids, hole-cutting and data transfers between overset grids have been especially designed for this type of mesh, where the Cartesian mesh is dominant and where curvilinear grids represent bodies in relative motion.

Here, unsteady Reynolds-Averaged Navier-Stokes equations (URANS) are solved, using Spalart-Allmaras turbulence model. 2<sup>nd</sup>-order accurate preconditioned AUSM scheme is used for Cartesian grids whereas Roe's scheme is applied on near-body grids. An implicit time integration using self-adaptive Newton method<sup>15</sup> is applied, with a maximum of 20 subiterations per time step.

Currently, rotor blades are resolved by near-body structured grids in relative motion with the Cartesian background grids. Unsteady Chimera transfers are applied at each subiteration of the time integration.

The fuselage can be either represented by a structured body-fitted mesh overlapping the off-body Cartesian mesh or by an immersed boundary within the Cartesian mesh. As the objective of this paper is to evaluate and compare Immersed Boundary Methods developed in Helios/ROAM and FAST/IBM for the capture of interactional aerodynamics of a rotorcraft configuration, the fuselage is represented by an Immersed Boundary.

FAST/IBM approach is a Ghost Cell Direct Forcing formulation, designed for attached turbulent boundary layers, as de-

scribed in details in Péron *et al.*<sup>6</sup>. This approach consists in marking cells as fluid or solid and forcing the solution at the fringe of solid points, in the close vicinity of the obstacles, such that the velocity is implicitly equal to zero at an immersed boundary describing a no slip boundary condition for instance.

In figure 2, the immersed boundary (black curve) tiles the domain into a solid region (left-hand side of the black curve) and fluid region (right-hand side). IBM forced or target points are the two layers of cells at the fringe of solid points (red dots).

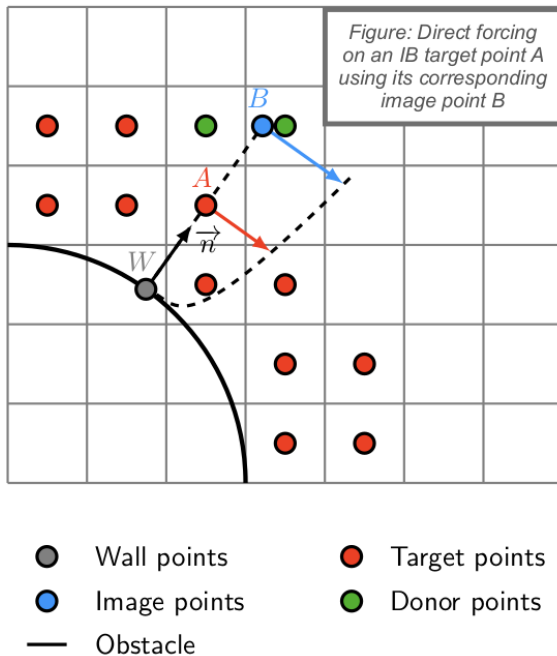


Figure 2: FAST/IBM approach: type of points used in the IBM reconstruction.

The IBM reconstruction needs an IB wall point (that is the projection of an IB target point onto the surface describing the immersed obstacle) and an IB image point (blue dot), the three of them being aligned along the wall normals. To update the solution at IBM target point  $A$  in red at a given iteration  $n$ , the solution at point  $B$  is used. As this point is not a discretization point, its solution is interpolated from its neighboring computed cells (donor points as green dots). Then, pressure and density defined at IB im-

age point  $B$  are set at IB target point. In the case of a turbulent boundary layer, the velocity at point  $A$  is obtained as follows: the friction velocity is computed at IB image point  $B$  and set at point  $A$  consequently. Then Musker's wall function is applied to reconstruct the tangential velocity at IB target point  $A$ . This wall function is algebraic and fits both the log layer and the viscous sub-layer. The normal velocity component is obtained by a linear reconstruction directly from the normal velocity at point  $B$ . The Spalart-Allmaras pseudo-viscosity at IB target points is also reconstructed (details can be found in the appendix of the paper<sup>6</sup>).

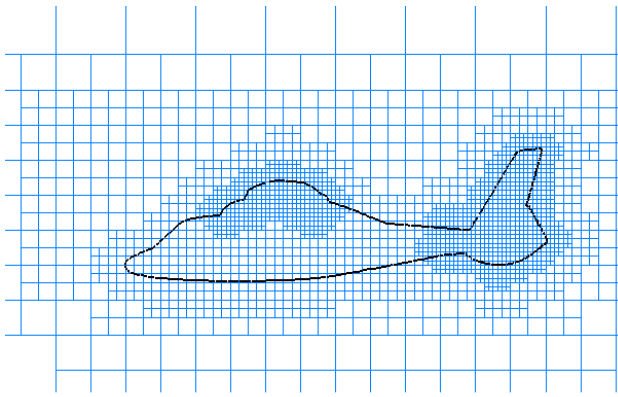
#### 4. SIMULATION OF THE ROTOR-FUSELAGE INTERACTION OF THE D365N CONFIGURATION

This section compares mid-fidelity simulations using FAST/IBM and Helios/ROAM with experimental results and three high-fidelity simulations. The three high-fidelity results are from Potsdam using OVERFLOW and Renaud using elsA in 2009<sup>8</sup>, using overset, structured curvilinear grids with low-Mach preconditioning for the fuselage. The last high-fidelity result is a recent result obtained using Helios mStrand without low-Mach preconditioning. The FAST/IBM simulation performed by ONERA is a URANS simulation using a wall-modeled IBM onto the fuselage and overset body-fitted grids for the blades. U.S. Army approach relies on Helios/ROAM, where the fuselage is also modeled by an immersed boundary, but without any wall function and an actuator line model for the rotor. A same spacing has been chosen for both simulations near the immersed boundary within the rotor wake in order to be comparable.

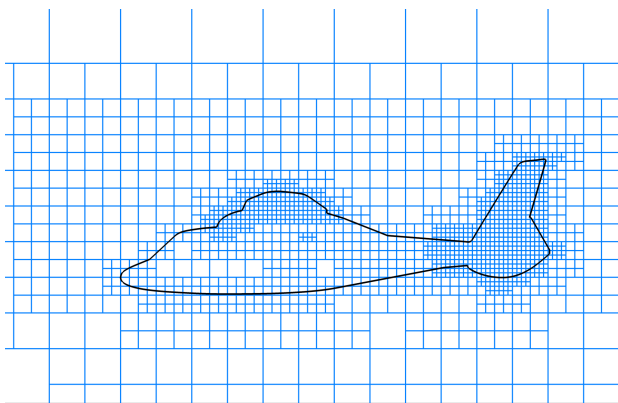
##### 4.1. Grid description

ROAM and FAST/IBM simulations rely on the same spacings in the vicinity of the fuselage

and around the rotor disk in order to compare the IBM approaches with the same near-wall resolution. A close-up view of the skeleton of the Cartesian mesh is represented in Figs. 3(a) and (b) for FAST/IBM and ROAM respectively.



(a) FAST/IBM



(b) Helios/ROAM

Figure 3: Octree skeleton of the Cartesian mesh for (a) FAST/IBM and (b) Helios/ROAM

Helios/ROAM skeleton tree is made of 33,386 octants, whereas FAST/IBM skeleton is made of 45,531 octants; indeed, the refinement levels close to the fuselage must be wide enough in the normal direction to the obstacle to maintain forced and image points in the same refinement level. Each octant is then filled with 16 points per direction, resulting in final Cartesian meshes made of 136.7 and 186.5 million points respectively. The finest cell is 0.977 m in the vicinity of the hub and the tail to represent sufficiently the sharp features of the geometry by the IBM. In other

regions close to the fuselage, the cell spacing is twice as big. For FAST/IBM approach, the actual distance to wall in wall unit  $y^+$  is around 100.

For FAST/IBM simulation, the four main rotor blades are meshed by a set of structured grids of 2 million points, overlapping the Cartesian mesh (Fig. 4).

Figure 5 shows the actuator line representation of the rotor blades results in clear high- and low-pressure regions in the background mesh, as shown by the red and blue areas.

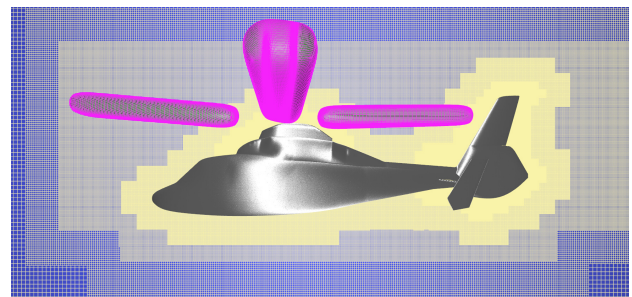


Figure 4: View of FAST/IBM mesh for the D365N configuration: four structured grids for each blade with the Cartesian mesh.

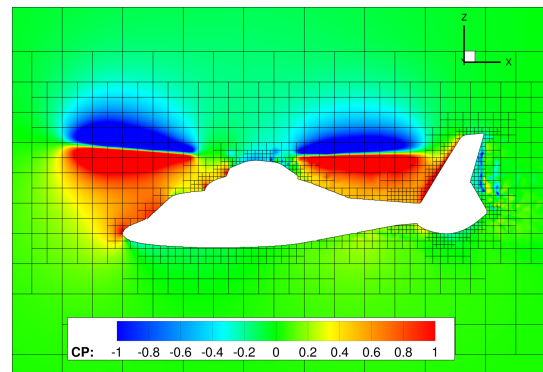


Figure 5: Helios/ROAM pressure contours (skeleton of the Cartesian mesh is represented).

#### 4.2. Rotor loads and wake visualization

The rotor thrust for Helios/ROAM and FAST/IBM simulations is compared to high-fidelity results using Helios with mStrand

(body-fitted solver) and reference overset results from Potsdam *et al* in 2009<sup>8</sup>. Experimental results from the F1 tunnel are also included for comparison<sup>8</sup>.

Time-averaged rotor thrust values are summarized in Table 1. FAST/IBM was run using two different time steps, the first one corresponding to a variation of azimuth per time step  $\Delta\Psi = 0.5^\circ$  and the second one to  $\Delta\Psi = 0.25^\circ$ . It has been observed that the variation of azimuth  $\Delta\Psi = 0.5^\circ$  leads to an underprediction of the thrust. Instead using  $\Delta\Psi = 0.25^\circ$  per time step seems to be a good compromise regarding the accuracy, which was also observed by Potsdam *et al.* for the high-fidelity simulations. All Helios simulations used a timestep of  $\Delta\Psi = 0.25^\circ$ .

	$\Delta\Psi$	$Z_b$
Helios ROAM	$0.25^\circ$	13.53
Helios mStrand	$0.25^\circ$	13.48
FAST/IBM	$0.5^\circ$	13.2
FAST/IBM	$0.25^\circ$	13.44
F1 exp	-	14.5
AFDD 2009	$0.25^\circ$	13.5
ONERA 2009	$0.25^\circ$	13.36

Table 1: Comparison of average rotor thrusts. The first four approaches are from the current work; the last three are from referenced work.

Figure 6 shows the rotor thrust over a full revolution of the rotor with averages shown as dotted lines. Despite a good agreement between all the simulations, they underpredict the experimental thrust of 10% roughly. The discrepancy may be due to assumptions made in HOST when trimming the rotor to obtain deflections for CFD. For consistency with previous high-fidelity results from 2009, the same rigid blade deflections were used and the rotor was not re-trimmed using CFD-CSD coupling. For the purposes of this work comparing mid- and high-fidelity results is more relevant than matching experimental results.

Figs. 7(a) and (b) display an isosurface of the Q criterion at  $Q = 11,548 s^{-2}$ , highlighting the impingement of the rotor wake on the fuselage. Compared to FAST/IBM, which has boundary-layer-resolved meshes, the actuator line method in Helios ROAM results in larger, diffused vortices trailing from the blade tips. The IBM methodology in Helios ROAM without a wall model results in flow separation on the fuselage and many small-scale flow features hitting the tail region. These small flow features are likely not physical, since they do not appear in the results from FAST/IBM or the high-fidelity results from Helios/mStrand or Potsdam *et al.*

Another deficiency of the ROAM actuator line method is poor resolution of the near-wake region behind the blade. At the same Q-criterion level the body-fitted blades solution from FAST/IBM shows a vortex sheet behind the blade. Since ROAM uses lifting line theory at discrete control points along the blade, the injection of source terms in the background mesh is not adequate to resolve span-wise gradients that result in the near-wake trailed vorticity.

The rotor and fuselage wake can be studied in further detail by analyzing vorticity at different planes of the background domain. Two planes were previously used for comparison against experimental PIV data in the work of Potsdam *et al.* Vorticity in the first plane, located at  $X = 1.52m$  behind the aircraft nose or  $(1.0125m$  behind the hub center), is shown in Fig. 8 for FAST/IBM and ROAM. The vortex structure is clearly asymmetric, as the blade root vortices visible in Fig. 7(a) coalesce on the left side of the fuselage and impact the horizontal tail. The ROAM solution from Fig. 8(b) shows many small-scale vortex structures behind the tail, as previously noted.

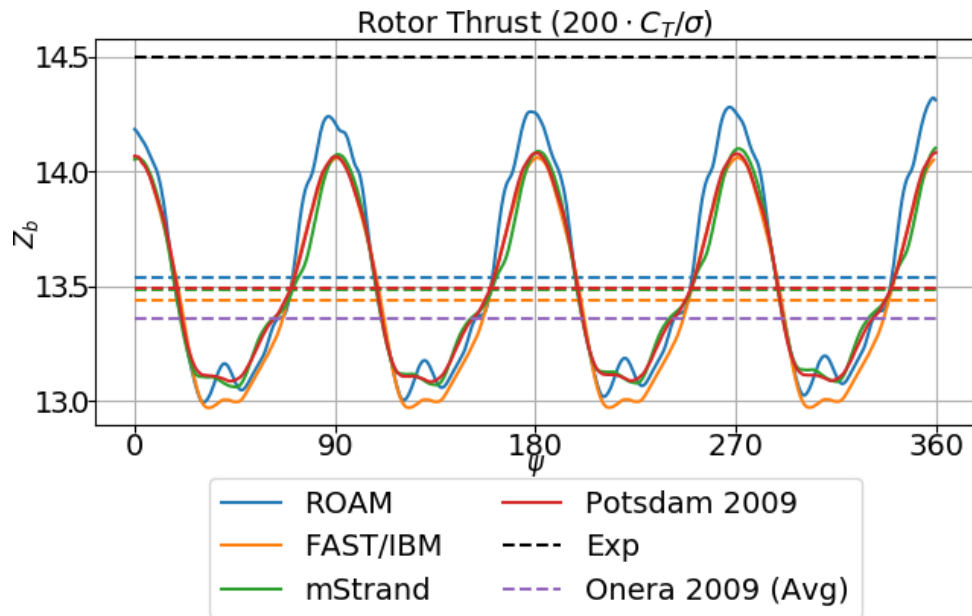
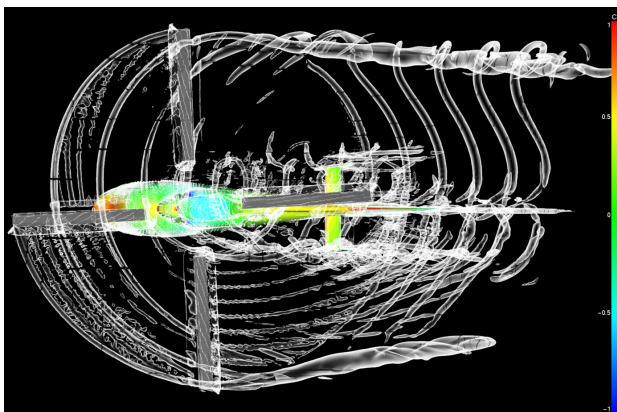
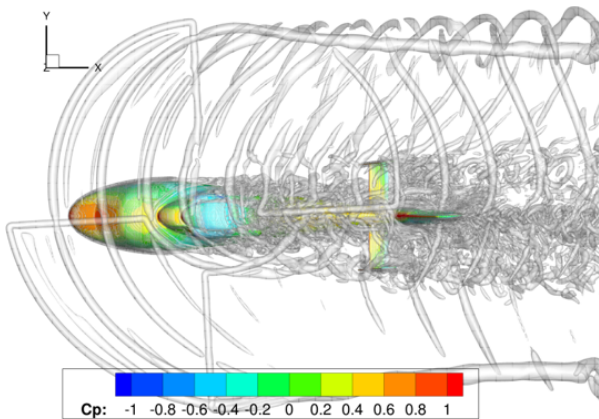


Figure 6: Comparison of rotor thrust between Helios/ROAM and FAST/IBM calculations against high-fidelity simulations and experiments.



(a) FAST/IBM

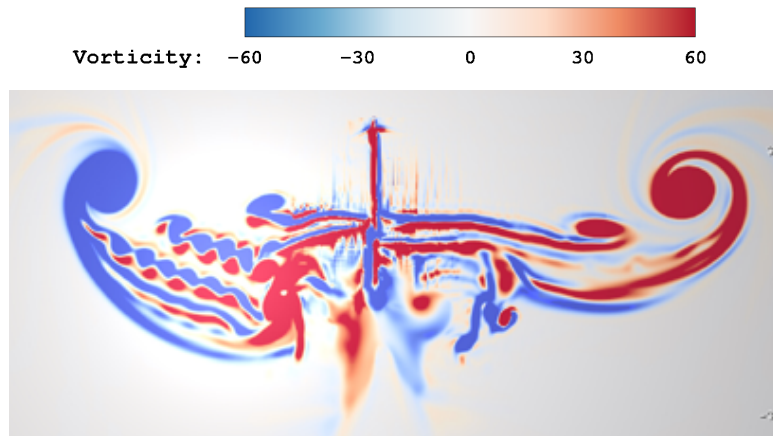


(b) Helios/ROAM

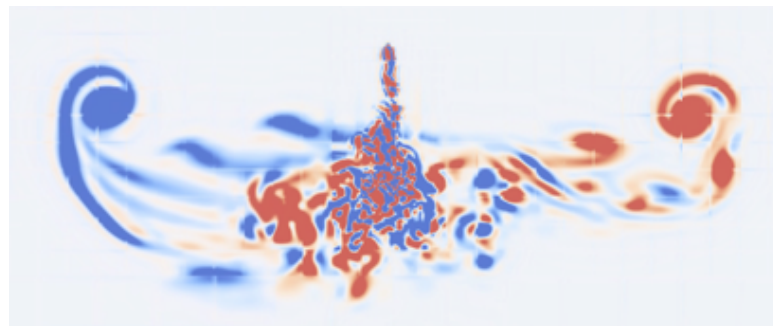
Figure 7: Isosurface of Q-criterion  $Q = 11548 \text{ s}^{-2}$  and pressure contours for (a) FAST/IBM and (b) Helios/ROAM.

The large rotor wake vortices on both the advancing and retreating sides of the aircraft are well captured by both solvers. The advancing (left) side has a stronger near-wake vorticity since the loads are distributed across the entire blade span. On the retreating (right) side the loads are more concentrated near the tip as a result of low relative velocity on the inboard sections of the blade. Since FAST/IBM has fully resolved blade meshes, the wake solution contains more clearly defined vorticity.

Figure 9 shows a  $Y = 0.475$  slice near the blade mid-span with contours of  $Y$ -vorticity on the retreating side of the aircraft. Again vorticity from Helios ROAM appears larger and more diffused compared to the tighter vortex structures from FAST/IBM. As the vortices convect behind the aircraft, the structures in FAST/IBM dissipate whereas with Helios/ROAM they maintain their strength longer. This is likely a result of the 2<sup>nd</sup> order spatial scheme used in FAST/IBM compared to the 5<sup>th</sup> order convective scheme in Helios.

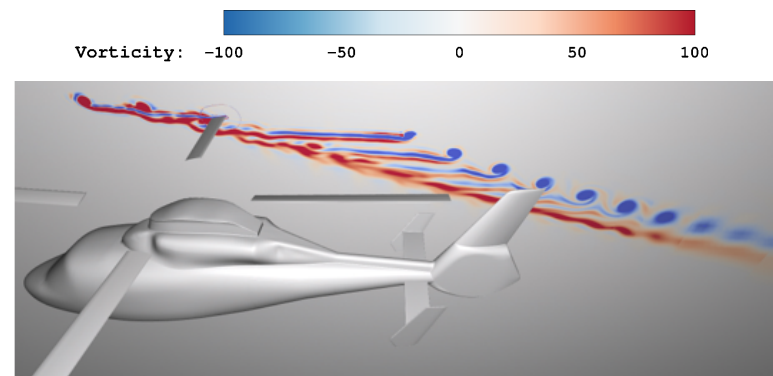


(a) FAST/IBM

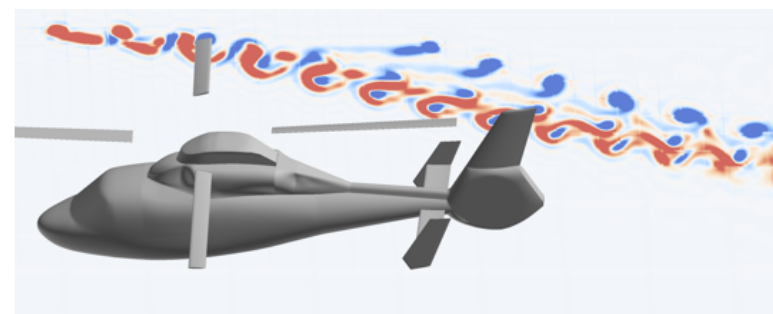


(b) Helios/ROAM

Figure 8: CFD wake  $X$ -vorticity ( $s^{-1}$ ) on plane  $X = 1.52\text{m}$  for (a) FAST/IBM and (b) Helios/ROAM.



(a) FAST/IBM



(b) Helios/ROAM

Figure 9: CFD wake  $Y$ -vorticity ( $s^{-1}$ ) on plane  $Y = 0.475\text{m}$  at the mid-span of the retreating blade for (a) FAST/IBM and (b) Helios/ROAM.

### 4.3. Fuselage forces

Figures 10(a) and (b) show the pressure reconstructed on the immersed surface and averaged over a quarter-revolution. The pressure is interpolated from the background mesh for ROAM, and using a Moving Least Squares reconstruction of pressure values at IBM target points for FAST/IBM. The centerline pressure coefficient is extracted and plotted along the upper-surface of the aircraft in Fig. 11. Stagnation pressures appear as red contours in the contour plot or spikes to  $C_P \approx 1$  in the centerline plot. Stagnation points appear in expected locations on the leading-edge surfaces of the fuselage. At the vertical tail, however, the pressure coefficient increases to well above 1, indicating an interaction from the main rotor.

The centerline pressure coefficients compare well between each of the methods. The aircraft geometry from Potsdam *et al.* include an additional cylindrical hub not present in the other simulations. The cylinder causes an additional stagnation point near  $X = 0.5$  and subsequent acceleration and pressure recovery behind the cylinder. Surprisingly one of the largest differences between results is between Helios mStrand and the Potsdam 2009 result, both of which are high fidelity simulations. The main difference is that mStrand did not use low Mach preconditioning on the fuselage. The Helios ROAM result in blue in Fig. 11 is shown with a light-blue band representing the min- and max- $C_P$  over the averaging interval. While Potsdam's 2009 result is an outlier compared to FAST/IBM, Helios ROAM and Helios mStrand, the red line roughly follows the min- $C_P$  range from Helios ROAM.

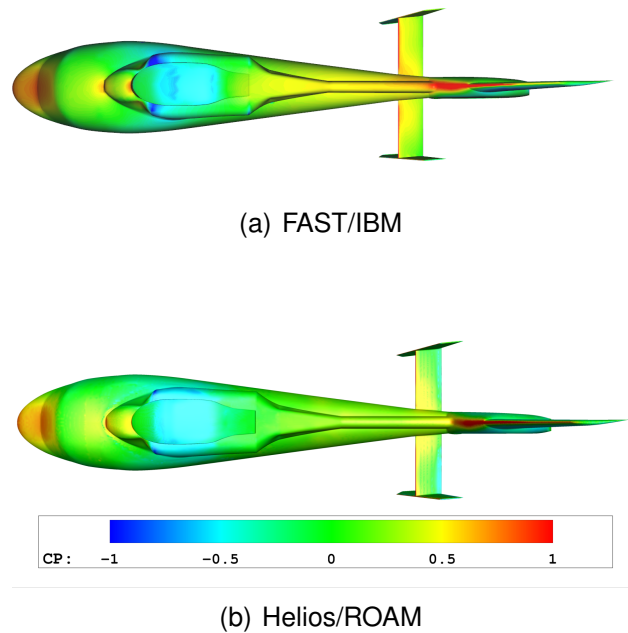


Figure 10: Time-averaged pressure coefficient on the fuselage.

Fuselage lift and drag are shown in Fig. 12 and Fig. 13 respectively. There is a clear 4/rev signature in the lift as a result of the download from the 4-bladed rotor. Results from FAST/IBM, Helios ROAM, and Potsdam *et al.* all agree quite well for lift, though values are higher than those from experiment. The Helios mStrand result is a bit of an outlier for fuselage lift; though values are closer to experiment, additional simulations using low Mach preconditioning should be used to ensure proper convergence of loads in low-Mach areas.

Fuselage drag predictions from FAST/IBM and Potsdam *et al.* agree quite well in both overall and oscillatory amplitudes. There is a slight 4/rev signal in the drag however not nearly as dominant as it was for lift. The 4/rev signal from Potsdam *et al.* is phase-shifted from the FAST/IBM result, indicating a possible limitation of the IBM approach. Interestingly both Helios mStrand and ROAM predict similar, higher drag compared to FAST/IBM and Potsdam *et al.*. As previously mentioned, mStrand

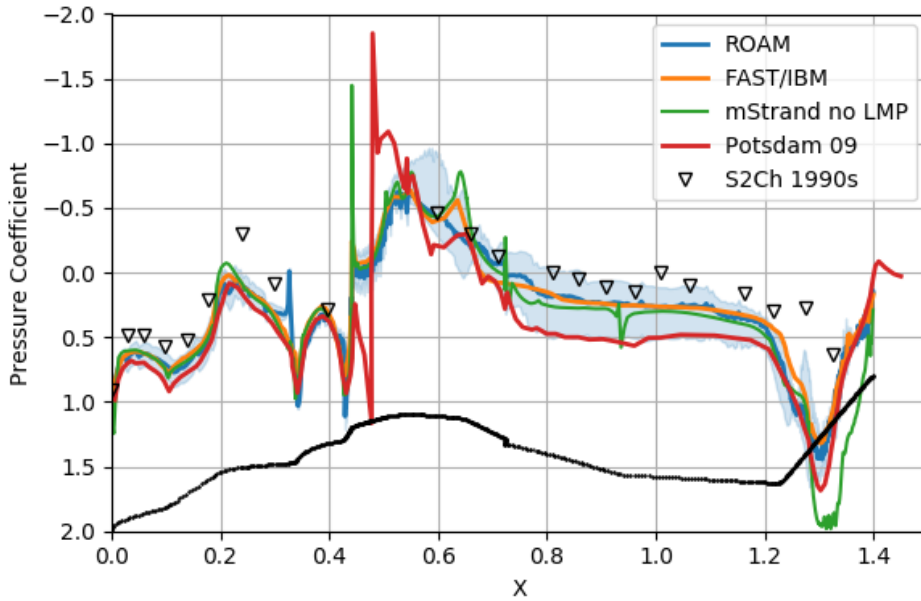


Figure 11: Time-averaged centerline pressure coefficient.

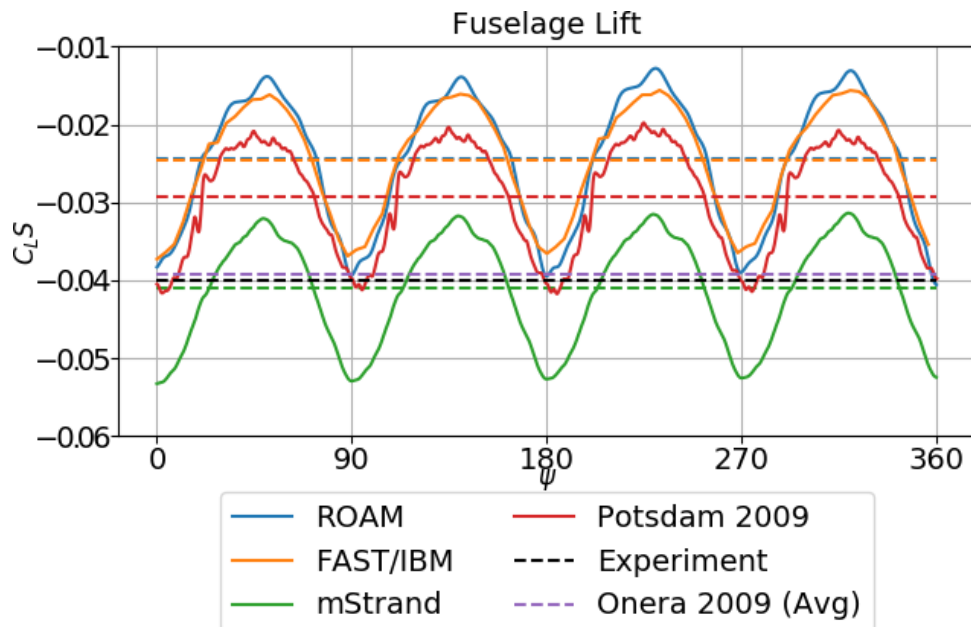


Figure 12: Comparison of fuselage lift between different approaches.

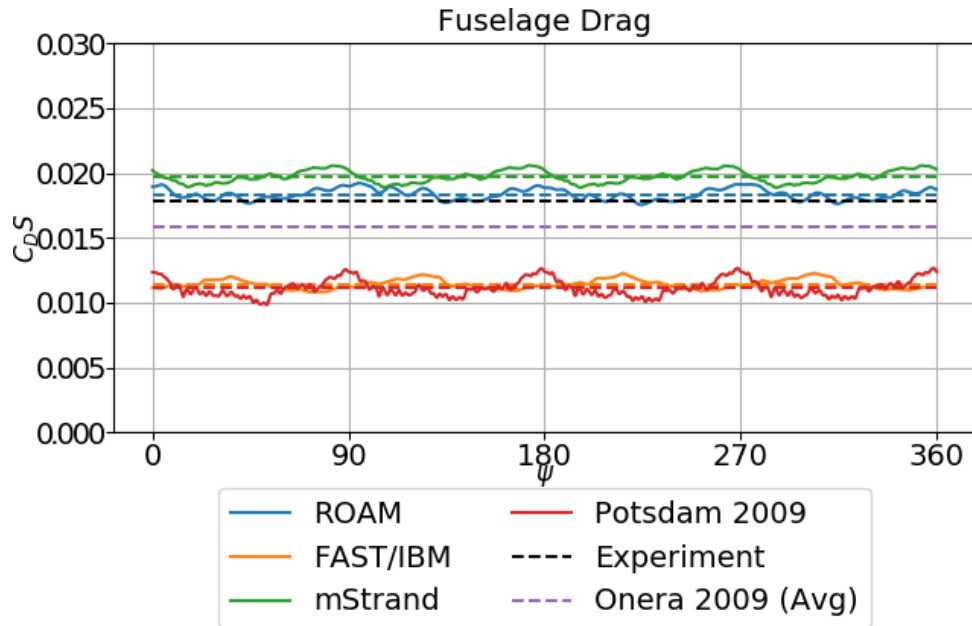


Figure 13: Comparison of fuselage drag between different approaches.

may be over-predicting drag as a result of no low-Mach preconditioning. ROAM is likely overpredicting drag as a result of the viscous-wall immersed boundary condition and non-physical separation observed in the Q-criterion plot from Fig. 7. Without a wall model ROAM does not correct the boundary condition to attain a turbulent boundary layer profile.

## 5. CONCLUSIONS

In this paper, an immersed boundary method (IBM) is assessed for the interactional aerodynamics between the rotor and the fuselage of a Dauphin helicopter in the frame of the US/France agreement on helicopters AHFIR.

This method has been developed recently both by ONERA and US Army on adaptive Cartesian grids, within FAST/IBM and Helios/ROAM frameworks respectively. This method enables to overcome the mesh generation effort as the mesh does not need to conform to obstacles; an immersed boundary condition (IBC) is applied to reconstruct implicitly the wall boundary condition. CFD simulations are performed using

a Cartesian solver that has proven efficient in terms of memory requirements and CPU time in comparison with curvilinear solvers.

Immersed boundary approaches are a good compromise between standalone low-fidelity tools and high-fidelity methods, the first ones usually lack the resolution necessary to capture interactions with the fuselage. Coupling low-fidelity tools with CFD for the fuselage to improve the accuracy of the prediction of the download can be achieved at the expense of generating a body-fitted mesh, which could be a tedious task for new configurations.

For that purpose, US Army approach consists in combining an actuator line model for the rotor with an immersed boundary for the fuselage within Helios/ROAM, whereas ONERA approach relies on a wall-modeled immersed boundary method coupled with overset grids for the rotor blades. It has been demonstrated that the interactional effects can be captured using both approaches: both approaches demonstrate the ability to capture the skin pressure coefficient over different parts of the body, showing reasonably good agreement with both the experiments and more computationally expensive

wall-resolved body-fitted CFD results. Analysis of the wake, especially in the vicinity of the empennage, demonstrates the capture of the interactional aerodynamics of this configuration. Helios/ROAM is not predicting the 4-per-rev signature of the fuselage drag as well as FAST/IBM. This is probably due to the immersed boundary method currently used ROAM which does not model the turbulent boundary layer, as opposed to the FAST/IBM approach which does through the application of a wall function at the IBM points on the fuselage.

In order to have at disposal tools of different fidelity, ONERA aims also at introducing a low-fidelity tool such as the actuator line model in ROAM to be combined with IBM. Future work will consist in applying the immersed boundary method onto a main rotor hub, for which the method should be well-suited as this kind of geometry can be complex and thus tedious to mesh using body-fitted approaches. The objective is to assess the capability of the IBM to predict the turbulent separated flows around geometrically complex parts of the rotorcraft. These validation studies will open the path to an efficient tool for helicopter download prediction of new configurations, with a good compromise between accuracy and process time.

## 6. ACKNOWLEDGMENT

The authors would like to acknowledge the support of the France-USA AHFIR cooperation represented by Arnaud Le Pape from ONERA side and Mark Potsdam and Rohit Jain from US Army side.

## REFERENCES

[1] Saberi, H., Hasbun, M., Hong, J., Yeo, H., and Ormiston, R., "RCAS Overview of Capabilities, Validations, and Applications to Rotorcraft Problems," American Helicopter Society 71st Annual Fo-

rum Proceedings, Virginia Beach, VA, 2015.

- [2] Benoit, B., Kampa, K., von Grunhagen, W., Basset, P.-M., and Gimonet, B., "HOST, a general helicopter simulation tool for Germany and France," Annual Forum Proceedings-American Helicopter Society, Vol. 56, 2000.
- [3] Cambier, L., Heib, S., and Plot, S., "The Onera elsA CFD software: input from research and feedback from industry," *Mechanics & Industry*, Vol. 14, (03), 2013, pp. 159–174.
- [4] Wissink, A. M., Jude, D., Jayaraman, B., Roget, B., Lakshminarayan, V. K., Sitaraman, J., Bauer, A. C., Forsythe, J. R., and Trigg, R. D., "New Capabilities in CREATE-AV Helios Version 11," AIAA SciTech 2021 Forum, jan 2021.
- [5] Jude, D., Sitaraman, J., and Wissink, A., "An octree-based, Cartesian Navier–Stokes solver for modern cluster architectures," *The Journal of Supercomputing*, Feb 2022.
- [6] Péron, S., Benoit, C., Renaud, T., and Mary, I., "An immersed boundary method on Cartesian adaptive grids for the simulation of compressible flows around arbitrary geometries," *Engineering with Computers*, 2020, pp. 1–19.
- [7] Constant, B. and Péron, S. and Beaugendre, H. and Benoit, C., "An improved Immersed Boundary Method for turbulent flow simulations on Cartesian grids," *Journal of Computational Physics*, 2021.
- [8] Potsdam, M., Smith, M., and Renaud, T., "Unsteady Computations of Rotor-Fuselage Interaction," European Rotorcraft Forum, 2009.
- [9] Mittal, A., Sreenivas, K., Taylor, L. K., and Hereth, L., "Improvements to the

- Actuator Line Modeling for Wind Turbines,” 33rd Wind Energy Symposium, 1 2015.
- [10] Churchfield, M. J., Schreck, S. J., Martinez, L. A., Meneveau, C., and Spalart, P. R., “An Advanced Actuator Line Method for Wind Energy Applications and Beyond,” 35th Wind Energy Symposium, January 2017.
- [11] Lakshminarayan, V. K., Sitaraman, J., Roget, B., and Wissink, A. M., “Development and validation of a multi-strand solver for complex aerodynamic flows,” *Computers & Fluids*, Vol. 147, 2017, pp. 41–62.
- [12] <https://w3.onera.fr/FAST>.
- [13] Benoit, C., Péron, S., and Landier, S., “Cassiopee: A CFD pre- and post-processing tool,” *Aerospace Science and Technology*, Vol. 45, 2015, pp. 272 – 283.
- [14] Péron, S. and Benoit, C., “Automatic off-body overset adaptive Cartesian mesh method based on an octree approach,” *Journal of Computational Physics*, Vol. 232, (1), 2013, pp. 153 – 173.
- [15] Daude, F., Mary, I., and Comte, P., “Self-Adaptive Newton-based iteration strategy for the LES of turbulent multi-scale flows,” *Computers and Fluids*, Vol. 100, 2014, pp. 278–290.